

# Towards a theory of attosecond transient recorder

E.E. Krasovskii<sup>1,2</sup> and M. Bonitz<sup>3</sup>

<sup>1</sup>*Departamento de Física de Materiales, Facultad de Químicas,  
Universidad del País Vasco, San Sebastián/Donostia, Basque Country, Spain*

<sup>2</sup>*Donostia International Physics Center (DIPC), San Sebastián/Donostia, Basque Country, Spain*

<sup>3</sup>*Institut für Theoretische Physik und Astrophysik, Universität Kiel, D-24098 Kiel, Germany*

Laser assisted photoemission by a chirped subfemtosecond extreme ultraviolet (XUV) pulse is considered within an exactly solvable quantum-mechanical model. Special emphasis is given to the energy dependence of photoexcitation cross-section. The streaked spectra are analyzed within the classical picture of initial time-momentum distribution  $r_{\text{ini}}(p, t)$  of photoelectrons mapped to the final energy scale. The actual time-momentum distribution in the absence of the probe laser field is shown to be a poor choice for  $r_{\text{ini}}$ , and a more adequate ansatz is suggested. The semiclassical theory offers a simple practically useful approximation for streaked spectra. Its limitations for sufficiently long chirped XUV pulses are established.

PACS numbers: 33.20.Xx, 33.60.+q

## I. INTRODUCTION

Subfemtosecond x-ray pulses are becoming a powerful tool for studying ultrafast processes in atoms [1, 2, 3] and solids [4], and their range of applications is growing rapidly [5]. The characterization of ultrashort pulses is an important problem in this field. The attosecond metrology is based on the laser assisted XUV (extreme ultraviolet) photoemission, whereby the temporal structure of the XUV pulse is reflected in the resulting streaked photoelectron spectrum [1, 2]. A subfemtosecond XUV pulse creates a photoelectron wave packet temporally confined within a fraction of the oscillation period  $T_L$  of the laser light. The wave packet is accelerated or decelerated by the superimposed laser field, and the dependence of the kinetic energy of the photoelectrons on the release time allows to record the time dependent spectra with a resolution around 100 as [3].

The gross features of the process can be understood within a quasi-classical model, in which the evolution of the photoelectron wave packet is split into two steps: first, a short XUV pulse creates an initial momentum distribution, which is then treated as a distribution of classical particles accelerated by the laser electric field. The model explains modulations of the width and center of gravity of the photoelectron spectra depending on the time delay of the laser pulse relative to the XUV pulse [1, 2]. Quantum-mechanical calculations of laser assisted atomic photoionization performed in Refs. [6, 7] have confirmed that the XUV pulse duration can be measured by the width modulation. Recently, various quantum-mechanical formalisms have been proposed that reveal the connection between temporal characteristics of the pump pulse and the streaked spectrum and form a basis for characterizing both the pulse and the electronic system being excited [8, 9]. Because the pump perturbation cannot be completely disentangled from the probe laser field the inverse problem – the reconstruction of the input pulse from the output spectra – is a difficult

one.

In Ref. [3] an XUV pulse of duration 250 as was first measured by the streaked photoelectron spectra from neon atoms, and it has been shown that the streaked spectrum can be treated as a tomographic image of the *initial time-momentum distribution of photoelectrons*. The two-step model has become a common paradigm in laser assisted photoemission [10, 11, 12]. Although the initial time-momentum distribution  $r_{\text{ini}}(p, t)$  appears to be an important concept in the theory of photoelectron streaking it is not straightforward to rigorously define this notion. A quantum-mechanical derivation of  $r_{\text{ini}}$  performed in Ref. [13] showed that under certain assumptions a function independent of the streaking field can indeed be constructed, and it reduces to the time-momentum distribution  $r_0(p, t)$  in the absence of the laser field. In Ref. [14] an alternative prescription for  $r_{\text{ini}}$  was introduced, which very satisfactorily described the streaked photoemission lineshape for a wide range of the XUV pulse durations and delay times. Understanding of the physical meaning and usage of the function  $r_{\text{ini}}(p, t)$  is important in order to correctly interpret the streaked spectra and obtain information about ultrafast electronic processes.

In the present paper the classical approach based on  $r_{\text{ini}}(p, t)$ , which hitherto has been used mainly for illustrative purposes, will be shown to have predictive power. We shall develop the semiclassical superposition approximation (SSA), in which the pump and the probe pulses can be disentangled. For a bandwidth-limited pump pulse it reduces the calculation of the final momentum intensity distribution of photoelectrons  $J(p)$  to the integral [14]

$$J(p) = \int_{-\infty}^{+\infty} U(t) I[p - \Delta p(t)] S[p - \Delta p(t)] dt,$$

where the shape of the pump pulse enters through its time intensity envelope  $U(t)$  and spectral intensity envelope  $I(p)$ , and the properties of the system enter through the excitation cross-section  $S(p)$ . The effect of the laser

field is described by the momentum  $\Delta p(t)$  transferred to the electron created at the time moment  $t$ . The choice of the integrand will be explained in Sec. IV A, and in Sec. V it will be extended to chirped pulses by replacing the function  $I(p)$  in the integrand by a function  $g(p, t)$  with an explicit time dependence:

$$J(p) = \int_{-\infty}^{+\infty} U(t)g[p - \Delta p(t), t]S[p - \Delta p(t)] dt.$$

We shall consider a one-dimensional prototype of the photoexcitation of an atom or a localized state at a solid state surface and apply the SSA to link the input to the output using the initial time-momentum distribution as an intermediary. The paper is organized as follows. The computational method is described in Sec. II. In Sec. III we analyze the time-momentum distribution of photoelectrons from a chirped pulse in the absence of the laser field. Section IV discusses laser dressed photoemission by non-chirped pulses: it reveals problems in defining the initial time-momentum distribution function  $r_{\text{ini}}$  and introduces a practical ansatz for  $r_{\text{ini}}$ . Section V generalizes SSA to chirped pulses and discusses the inverse problem.

## II. MODEL PARAMETERS AND METHOD

In order to avoid any numerical approximations in solving the time-dependent Schrödinger equation we employ the one-dimensional model adopted in Ref. [14]. The unperturbed Hamiltonian (in the units  $\hbar = 1$ ,  $m = 1/2$ ) is  $\hat{H} = -\Delta + V(z)$ . The model potential  $V(z)$  is a piecewise constant function shown in Fig. 1(a). The system is enclosed in a box, so that the spectrum of  $\hat{H}$  is discrete. This setup describes the photoemission from a localized atomic state in a crystal close to the surface. We shall consider the lowest state of the model atom [ $\epsilon_i = -18.1$  eV, see Fig. 1(b) and the figure caption]. The XUV pulse creates two wave packets traveling in opposite directions. We shall consider the spectrum of the one traveling to the right. Although the presence of the surface barrier between bulk and vacuum, see Fig. 1(a), is not essential for the present application, the barrier is retained for technical convenience: it reduces the total number of energy levels and slows down the right traveling packet.

The electric field  $E(t)$  applied to the system is a superposition of the XUV (subscript X) and laser (L) pulses:

$$E(t) = E_X(t - t_X) \cos[\omega_X(t - t_X)] + E_L(t - t_L) \sin[\omega_L(t - t_L)].$$

The XUV and the laser pulse are confined to the intervals of length  $D_X$  and  $D_L$  centered at  $t_X$  and  $t_L$ , respectively, and their envelopes  $E_X$  and  $E_L$  have the same shape

$$E_{X,L}(t) = E_{X,L}^0 \cos^2 \frac{\pi t}{D_{X,L}} \quad \text{for } t \in \left[ -\frac{D_{X,L}}{2}, \frac{D_{X,L}}{2} \right],$$

see Fig. 1(c). Note that  $D_{X,L}$  are twice the FWHM duration often used in the literature. The intensity spectrum

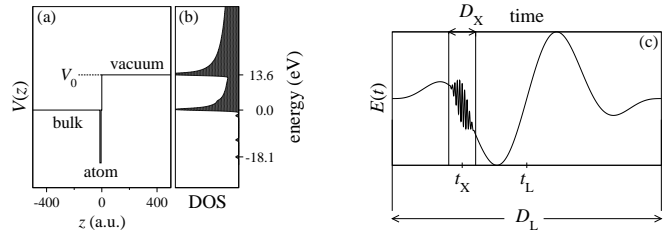


FIG. 1: (a) Potential  $V(z)$  of the model 1D system. The atom is represented by a 6 a.u. wide potential well centered at  $z = -8$  a.u. relative to the surface barrier. (b) Density of states. (c) Superposition of the electric field of the XUV pulse of duration  $D_X$  and the laser pulse of duration  $D_L$ .

$I(\omega)$  of such XUV pulse is close to Gaussian. To construct the classical model we shall need the normalized temporal intensity envelope of the XUV pulse  $U(t)$  defined by the formula

$$U(t) = [E_X(t)/E_X^0]^2. \quad (1)$$

All calculations are performed for  $\omega_X = 91$  eV and  $E_X^0 = 10^6$  V/cm, which is within the perturbational limit. We shall also consider linearly chirped pulses, with  $\omega_X$  changing in time:

$$\omega_X(t) = \omega_X^0 + b(t - t_X). \quad (2)$$

The parameters of the laser pulse applied to the system are typical of attosecond spectroscopy [15]: all calculations are performed for frequency  $\omega_L = 1.65$  eV ( $T_L = 2.5$  fs) and duration  $D_L = 5$  fs. In the following we set the center of the laser pulse to zero,  $t_L = 0$ . If not otherwise stated the laser field amplitude is  $E_L^0 = 6 \times 10^7$  V/cm.

The perturbation in dipole approximation is  $zeE(t)$ , and the time-dependent Schrödinger equation (TDSE) is solved in matrix form in terms of exact eigenfunctions of  $\hat{H}$ . In spite of its simplicity the model is quite realistic. In particular, the energy variations of the excitation cross-section are in accord with those experimentally observed, see Ref. [14]. A more sophisticated development of the model has been recently applied to laser assisted photoemission from solids [16]. The wave packets created by the XUV pulse can be driven back to the ion and rescatter, thereby absorbing additional UV photons. This was studied for ionization in Ref. [17] and for electron scattering on an ion in Ref. [18] by solving the TDSE for a 1D and 2D model system. In the present work we are interested in the energy distribution  $J(\epsilon)$  of photoelectrons recorded by a detector far away from the excitation region. The spectrum  $J(\epsilon)$  is calculated by reexpanding the packet moving to the right in terms of the eigenfunctions of the system.

We shall adopt the following convention about notation. The three variables – energy  $\epsilon$ , momentum  $p$ , and frequency (XUV photon energy)  $\omega$  – can be used one instead of another as argument of frequently used functions. They are simply connected:  $\omega = \epsilon - \epsilon_i$ , with

$\epsilon_i$  being the energy of the photoemission initial state;  $\epsilon = p^2 + V_0$ . The kinetic energy of the photoelectron in vacuum is, thus,  $\epsilon_i + \omega - V_0$ . For the sake of brevity, we shall use  $\epsilon$ ,  $p$  or  $\omega$  depending on the context, e.g.,  $J(\omega)$  is the short for  $J(\omega + \epsilon_i)$ , and  $J(p)$  is the short for  $J(p^2 + V_0)$ .

### III. XUV EMISSION WITHOUT LASER FIELD

The temporal evolution of the photoelectron spectrum during the XUV pulse is shown in Fig. 2 for a bandwidth limited and for linearly chirped pulses. The color map shows the time and energy dependent occupation number  $J(\epsilon, t)$  of eigenstates  $|\epsilon\rangle$ . The vertical cross section of the map at the end of the pulse  $J(\epsilon, t_x + \frac{1}{2}D_x) \equiv J(\epsilon)$  is the energy distribution curve (EDC) measured in the experiment. The time derivative of the function  $J(\epsilon, t)$  gives the energy resolved transition rate

$$r_0(\epsilon, t) = dJ(\epsilon, t)/dt. \quad (3)$$

The function  $r_0(p, t)$  is, thus, the time-momentum distribution of photoelectrons in the absence of the laser field.

In the absence of the laser field the observed final EDC obeys the simple formula [14]:

$$J(\epsilon) \sim I(\epsilon)S(\epsilon), \quad (4)$$

where  $I(\omega)$  is the spectral intensity distribution of the XUV pulse, and  $S(\epsilon)$  is the photoemission cross-section,

$$S(\epsilon) = |\langle \epsilon | z | \epsilon_i \rangle|^2. \quad (5)$$

Equation (4) predicts the photoelectron spectrum without solving the TDSE. It is a consequence of the weak XUV perturbation and of the negligible probability of transitions within the (quasi-) continuum,  $\epsilon > 0$ , see Appendix. (This relation is also obtained in the perturbational limit of the approximation to the TDSE introduced by Lewenstein *et al.* [19], i.e., in the limit when the vector potential of the electric field can be neglected compared to the electron momentum.) For the present system it is found to hold for XUV pulses over a wide range of pulse parameters. Also the entire map  $J(\epsilon, t)$  calculated from Eq. (4) practically coincides with the exact result.

The spectrum evolution is seen to strongly depend on the chirp rate. The effect of a linear chirp on the intensity spectrum can be characterized by the dimensionless index  $\eta = bD_x/\Gamma_x^0$ , where  $\Gamma_x^0$  is the full spectral width at half maximum (FWHM) of the non-chirped pulse with the same envelope and the carrier frequency  $\omega_x^0$ . When  $\eta$  approaches 4 the  $J(\epsilon, t)$  map starts acquiring a characteristic stripe structure, see Fig. 2(b,c,f). However, it is not straightforward to determine the value of the chirp rate from a known  $J(\epsilon, t)$  distribution.

To illustrate the point, we show in Fig. 3 the time dependence of the center of gravity of the EDC  $\epsilon_g(t)$  obtained by integrating along vertical lines in the transition

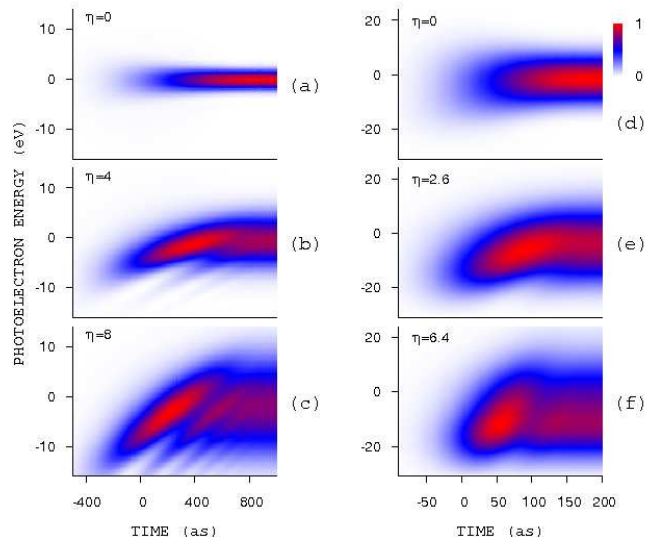


FIG. 2: (color online) Time dependent occupation of final states  $J(\epsilon, t)$  for the duration  $D_x = 2000$  as,  $\Gamma_x^0 = 3$  eV (left column) and 400 as,  $\Gamma_x^0 = 15$  eV (right column). The chirp rate  $b$  is zero in graphs (a) and (d), and  $b = 6$  (b), 12 (c), 96 (e), and 240 eV/fs (f). The photoelectron energy is given relative to  $\epsilon_i + \omega_x^0$  [the frequency at  $t = 0$  is  $\omega_x^0 = 91$  eV, see Eq. (2)] and time relative to  $t_x$ . The maximum intensity is set to 1. The vertical cross section at the right border of the map is the final intensity distribution  $J(\epsilon)$  recorded by the detector.

rate map, see Fig. 2. The function  $\epsilon_g(t)$  has a complicated form with variable slope, which depends not only on the photon energy sweep  $b$  but also on the pulse duration. The fact that  $b$  cannot be immediately inferred from  $d\epsilon_g(t)/dt$  is a combined effect of two factors: the FWHM of the EDC changes with time, and the broader the EDC the stronger it is affected by the energy dependence of the cross-section  $S(\epsilon)$ . In the present example the cross-section is higher at lower energies, see right panel of Fig. 3, so the broader the frequency distribution

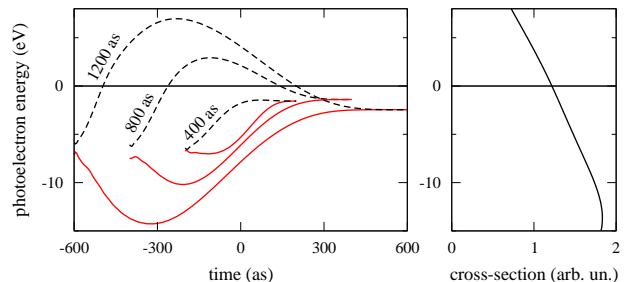


FIG. 3: (color online) Time dependence of the photoelectron spectrum center of gravity  $\epsilon_g(t)$  for the chirp rate  $b = \pm 24$  eV/fs for three pulse durations:  $D_x = 400, 800,$  and 1200 as. Positive (negative) chirp is shown by full (dashed) lines. Right panel shows the function  $S(\epsilon)$ , see Eq. (5). Photoelectron energy  $\epsilon$  is given relative to  $\epsilon_i + \omega_x^0$ .

the larger the downward shift of the center of gravity. This produces a different effect on the spectra depending on the sign of the chirp, so the curves for opposite chirps in Fig. 3 are not symmetric. At  $t = D_x/2$  the curves of opposite chirp converge, which follows from Eq. (4) because the spectrum  $I(\omega)$  of a linearly chirped pulse does not depend on the sign of chirp.

The function  $J(\epsilon, t)$  is the most fundamental quantity that contains information about the details of the ionization process. In the simple case considered above the properties of the system enter via the energy dependent cross-section  $S(\epsilon)$ , and its structure is seen to be reflected in  $J(\epsilon, t)$ . At the same time, this means that in general the XUV pulse cannot be satisfactorily characterized by gross features of the resulting photoelectron spectrum evolution. In addition, the function  $J(\epsilon, t)$  cannot be directly measured in an experiment, which makes the problem of disentangling the pulse characteristics from the properties of the system highly nontrivial. The only way to probe  $J(\epsilon, t)$  is the laser streaking technique, which we consider in the next section.

#### IV. EFFECT OF LASER FIELD ON LINESHAPE

Let us consider photoelectrons emitted parallel to the electric field of a linearly polarized light. They are accelerated or decelerated depending on the sign of the momentum transfer  $\Delta p(t) = (e/c)A(t)$  from the laser field to an electron created at the time  $t$ . As a result, the spectrum shifts as a whole on the kinetic energy scale and distorts. One reason for the distortion is a finite width of the photoelectron spectrum: electrons with different momenta  $p$  acquire different energies, so the spectrum broadens when accelerated and narrows when decelerated. Another source of distortion is the finite duration  $D_x$  of the XUV pulse: electrons created at different moments  $t$  are differently accelerated according to the current value of the momentum transfer  $\Delta p(t)$ .

##### A. Initial time-momentum distribution

In the absence of the laser field the momentum distribution of photoelectrons  $J(p)$  after the XUV pulse is over can be expressed as the integral of the transition rate:

$$J(p) = \int_{t_x - \frac{1}{2}D_x}^{t_x + \frac{1}{2}D_x} r_0(p, t) dt.$$

This formula can be generalized to the case of laser assisted photoemission by considering  $J(p)$  as a projection of the initial time-momentum distribution onto the scale of final momenta  $p$ , which is the essence of the classical

picture of the streaking measurement [3]:

$$J(p) = \int_{t_x - \frac{1}{2}D_x}^{t_x + \frac{1}{2}D_x} r_{\text{ini}}[p - \Delta p(t), t] dt. \quad (6)$$

This equation means that the electron created at a moment  $t$  in the state  $p - \Delta p(t)$  is brought by the laser field to the final state  $p$ , and all such processes at different moments  $t$  during the action of the XUV pulse are summed up incoherently.

Let us concentrate on the physical meaning of the function  $r_{\text{ini}}(p, t)$ . This function characterizes the XUV pulse, and at the same time it depends on the properties of the electronic system. To define this function requires a separation of the XUV and the laser pulses, which is, in general, not possible. For example, the time-momentum distribution in the absence of the laser field  $r_0(p, t)$  cannot serve this purpose. First, even in the simplest case of a bandwidth limited pulse, for momenta far enough from the central momentum the function  $r_0(p, t)$  becomes negative because the momentum distribution of photoelectrons narrows with time. This is illustrated by the dot-dashed line in Fig. 4(a), which shows two examples of  $r_0(p, t)$  calculated by the TDSE. The implication for the laser assisted photoemission is shown in Fig. 5, which compares exact streaked spectra from the TDSE with those from the SSA. Although the contribution from negative values of  $r_0$  is small it is not negligible, which is seen by the negative values of the spectral intensity in the dashed curves in Fig. 5. More important is that also around the central momentum, for which  $r_0$  is everywhere positive [dashed line in Fig. 4(a)], it provides a rather inaccurate final distribution  $J(p)$  (compare dotted and dashed lines in Fig. 5).

Instead of  $r_0$  we can use in Eq. (6) the separable ansatz

$$r_{\text{ini}}(p, t) \rightarrow U(t)I(p)S(p) \quad (7)$$

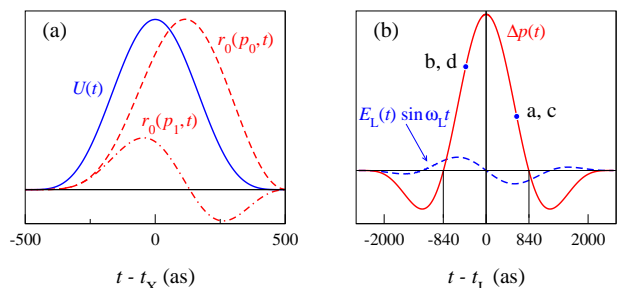


FIG. 4: (color online) (a) Temporal intensity profile of the XUV pulse envelope  $U(t)$ , see Eq. (1), (solid line) compared to the laser-free transition rate functions  $r_0(p, t)$  for the central momentum,  $p_0^2 = \epsilon_i + \omega_x - V_0$  (dashed line), and for a momentum far from the center  $p_1$  (dot-dashed line). (b) Electric field  $E_L(t)$  of the laser pulse (dashed line) and the transferred momentum  $\Delta p(t)$ . The circles indicate the release points  $t_x$  of the XUV pulses studied in Fig. 5.

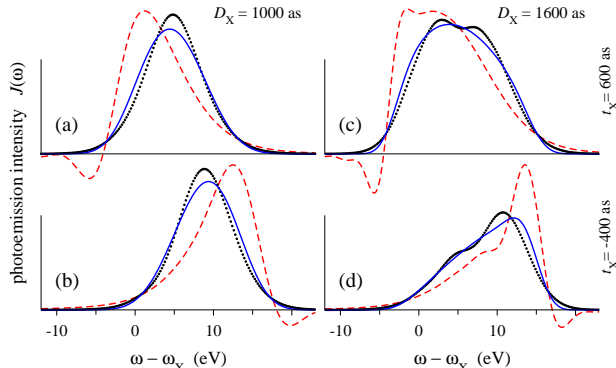


FIG. 5: (color online) Streaked photoelectron EDCs for XUV pulse durations  $D_x = 1000$  as (a, b) and  $1600$  as (c, d) and release points  $t_x = 600$  as (a, c) and  $-400$  as (b, d) indicated in Fig. 4(b). Dotted lines are the full solution of the TDSE, and solid lines are obtained from the SSA equation (6) with the function  $r_{\text{ini}}$  from Eq. (7). Dashed curves result from using the laser-free function  $r_0$  in Eq. (6).

introduced in Ref. [14], which turns out to perform much better, see solid lines in Fig. 5. In the phenomenological formula (7) the explicit time dependence of the initial time-momentum distribution comes solely through the temporal intensity envelope  $U(t)$  of the XUV pulse [see Eq. (1)], which is shown by the solid line in Fig. 4(a). (Oscillations with the frequency  $\omega_x$  are, thus, completely ignored.) In the presence of the laser field the functions  $I$  and  $S$  in Eq. (6) also depend on time through the argument  $p - \Delta p(t)$ . The formula (7) establishes a simple connection between the structure of the XUV pulse and the streaked photoelectron spectrum, and it can be useful for the characterization of the pulse provided it reasonably simulates the true spectrum. It satisfies the two limiting cases: first, for an extremely short pulse,  $\Delta p(t)$  can be considered constant, and Eqs. (6)–(7) yield a shift of the spectrum as a whole. Second, in the absence of the laser field the equation (4) is recovered.

Figure 4(a) compares laser-free functions  $r_0(\epsilon, t)$  with the function  $U(t)$  used in the ansatz (7). At the Fermi golden rule energy  $\epsilon_i + \omega_x$  the true population profile  $r_0$  is retarded by some 100 as with respect to the XUV intensity profile  $U(t)$ , which is sufficient to cause an error of more than 3 eV in the location of the spectral maximum. At the same time, equation (6) with the heuristic ansatz (7) reproduces the spectra with a surprisingly high quality (compare dotted and solid lines in Fig. 5). Thus, in view of the sensitivity of the streaked spectra to small details of the function  $r_{\text{ini}}(\epsilon, t)$ , the prescription (7) appears to be a reasonable choice. The model performs well for durations well exceeding a linear interval of the  $\Delta p(t)$  function. It describes the dependence of the spectral width on release point and pulse duration, as well as the asymmetric shape of the streaked EDCs [see Fig. 5(d)].

## B. Effect of a rapid change of momentum transfer

A detailed discussion of the laser field induced line-shape variations of photoemission spectra has been presented in Ref. [14]. We shall now consider the possibility of inferring the XUV pulse duration from the measured streaked EDC. At a point where  $\Delta p(t)$  rapidly changes with time, electrons created at different moments  $t$  are differently accelerated according to the current value of  $\Delta p(t)$ , so the longer the pulse is, the stronger the EDC broadens. This “temporal” broadening is accompanied by the energy stretch of the spectrum due to a uniform shift along the  $p$  axis (electrons with higher kinetic energies acquire larger energy from the laser field than those with lower energies). If the integral momentum transfer can be neglected [around  $t - t_L = \pm 840$  as, see Fig. 4(b)] the latter effect is minimal. It has been suggested in Ref. [3] that in this case the temporal emission profile  $U(t)$  is uniquely mapped into a spectral distribution of photoelectrons  $J(\epsilon)$ , and temporal information can be retrieved from a single streak record.

Owing to the finite spectral width of the XUV pulse the streaking broadening  $\Delta \Gamma_e$  (i.e., the difference between the FWHM of the photoelectron spectra in the presence and in the absence of the laser field) depends on the pulse duration  $D_x$  in a complicated manner. Figures 6(a,b) show the dependence of  $\Delta \Gamma_e$  on  $D_x$  for two release points  $t_x$  and three laser field intensities. Up to durations well exceeding the linear interval of  $\Delta p(t)$  the streaking broadening steadily increases with  $D_x$  while the FWHM of the field-free spectrum steadily decreases. As a result, two different temporal profiles  $U(t)$  may give almost identical streaked spectra.

The duration can, however, be immediately inferred

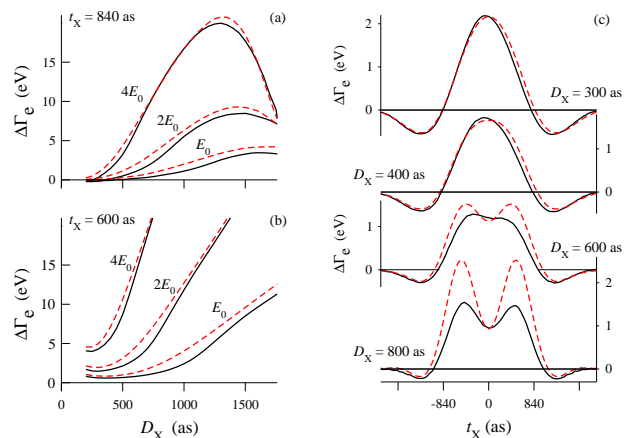


FIG. 6: (color online) Graphs (a) and (b) show the dependence of the streaking broadening  $\Delta \Gamma_e$  on the duration  $D_x$  of the XUV pump pulse for two release points  $t_x = 840$  as (a) and  $600$  as (b) by the full solution of the TDSE (solid lines) and by the SSA (dashed lines). The curves are presented for three values of the laser field amplitude:  $E_0 = 6 \times 10^7$  V/cm, as well as  $2E_0$  and  $4E_0$ . Graph (c) shows the dependence of  $\Delta \Gamma_e$  on release time for  $D_x = 300, 400, 600,$  and  $800$  as.

from  $\Delta\Gamma_e$ , and the SSA gives a reasonable approximation over a wide range of laser intensities. For small  $D_x$  the width of the non-streaked spectrum increases, and the absolute values of  $\Delta p(t)$  start playing a more important role: the energy stretch (which varies in time) interferes with the temporal broadening. At the release point  $t_x = 600$  as the integral momentum transfer is much larger, so the energy stretch at small  $D_x$  leads to the presence of a minimum in the  $\Delta\Gamma_e(D_x)$  curve.

At short durations, the streaking broadening not only becomes small at the point of zero momentum transfer, but also the sensitivity of  $\Delta\Gamma_e$  to the release point increases, as illustrated by Fig. 6(c). This means that this point is less favorable for the measurement of  $D_x$  than the measurement at the point of maximal momentum transfer. Figure 6(c) suggests that  $\Delta\Gamma_e$  measured at  $t_x = 0$  (maximum  $\Delta p$ ) and  $t_x = \pm 1250$  as (minimum), as well as the  $t_x$  location of the extrema would characterize the XUV pulse more accurately.

Figure 6 shows that the results by the SSA (6)–(7) closely follow the exact solutions (except for the overestimated maximal broadening for longer pulses), and their quality does not deteriorate with increasing the streaking field strength.

## V. EXTENSION OF SSA TO CHIRPED PULSES

We now generalize the semiclassical approach to chirped pulses. We again rely on Eq. (6) to separate the pump and probe pulses, but Eq. (7) is not applicable now because it cannot discriminate between positive and negative chirp. Indeed, the pump pulse enters through its spectrum  $I(\omega)$  and time envelope  $U(t)$ , while both functions do not depend on the sign of the chirp rate  $b$  [defined in Eq. (2)]. In order to include the photon energy sweep in our model we must ascribe physical meaning to the formal notion of instantaneous frequency  $\omega_x(t)$ . Thereby the spectral intensity distribution  $I(\omega)$  in Eq. (7) will acquire an *explicit* time dependence. To achieve this we introduce an ‘instantaneous’ spectral intensity distribution  $g(\omega, t)$ . In order to satisfy the basic equation (4) in the absence of the laser field, this function should obey the relation

$$I(\omega) = \int_{-\infty}^{+\infty} g(\omega, t)U(t) dt. \quad (8)$$

For a linear chirp and a temporal intensity distribution of Gaussian form,  $U(t) \sim \exp[-(16 \ln 2) t^2/D_x^2]$ , the spectral intensity distribution  $I(\omega)$  is again a Gaussian with FWHM  $\Gamma_x = [64(\ln 2)^2 + D_x^4 b^2]^{1/2}/D_x$ , and equation (8) has the explicit solution:

$$g(\omega, t) = \exp\left[-\frac{(\omega - \omega_x^0 - bt)^2}{\gamma^2/4 \ln 2}\right], \quad \gamma^2 = \Gamma_x^2 - \frac{D_x^2 b^2}{4}. \quad (9)$$

Although in our case the function  $U(t)$  deviates from Gaussian we shall employ this form of  $g(\omega, t)$  and the

requirement that the convolution (8) yield the FWHM  $\Gamma_x$  of the actual spectral distribution  $I(\omega)$ .

The semiclassical superposition (6) with the ansatz

$$r_{\text{ini}}(p, t) = U(t)g(p, t)S(p) \quad (10)$$

for the initial momentum distribution takes into account both the temporal and the spectral structure of the pump pulse. Thus, from the point of view of photoemission, the pump pulse is thought to produce at the time point  $t$  transitions with the spectral intensity distribution proportional to  $g(\omega, t)$  [centered at  $\omega_x(t)$ ] and the maximal intensity proportional to  $U(t)$ . In the limit of zero chirp, according to the requirement (8), the function  $g(\omega, t)$  becomes time independent and reduces to  $I(\omega)$ , which leads back to Eq. (7). Note that in contrast to the pulselet representation of Ref. [8], the function  $g(\omega, t)$  does not contain phase, and its width is much smaller than the spectral width of a pulselet.

Let us see how well the SSA (6) with the initial distribution (10) describes the dependence of the streaking broadening  $\Delta\Gamma_e$  on the chirp rate  $b$  of the pump pulse. For  $b = 0$  the broadening  $\Delta\Gamma_e$  as a function of  $t_x$  is practically symmetric with respect to  $t_x = 0$ , see Fig. 6(c). For long pulses the ‘temporal’ broadening mechanism dominates, and the curve  $\Delta\Gamma_e(t_x)$  has two distinct maxima (which merge into a broad one at  $t_x = 0$  when the duration decreases). The symmetric shape is completely

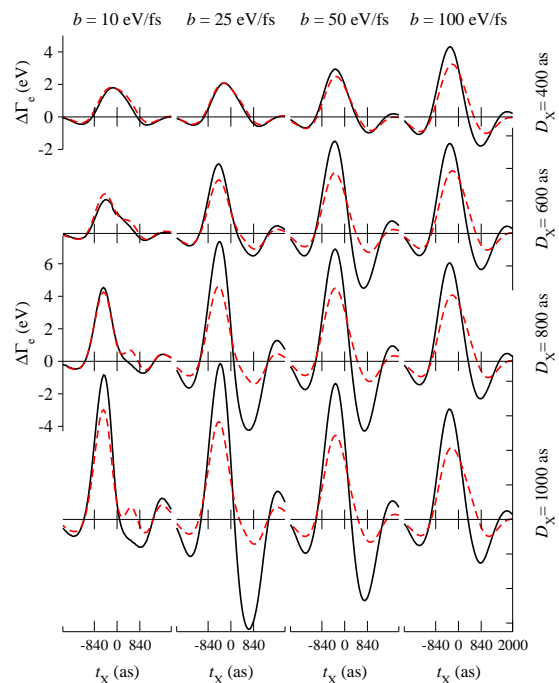


FIG. 7: (color online) Dependence of the streaking broadening  $\Delta\Gamma_e$  of the photoelectron spectra on the release point  $t_x$  for four values of chirp rate  $b = 10, 25, 50,$  and  $100$  eV/fs and four pulse durations  $D_x = 400, 600, 800,$  and  $1000$  as. Solid lines are the exact solution of the TDSE and (red) dashed lines are obtained from the SSA equations (6) and (10).

distorted already at small chirp rates, see Fig. 7. One of the maxima is strongly damped and the other one is enhanced, so the shape of the curve provides a signature of the temporal structure of the XUV pulse.

At a zero momentum transfer point the photoelectron spectrum excited by a positively chirped pulse is stretched by the positive and compressed by the negative laser field. This means that from the measured  $\Delta\Gamma_e$  at the two  $t_x$  points one can infer both the duration and the chirp of the pump pulse [3]. Indeed, Fig. 7 shows that both the broadening and the compression steadily increase with the pulse duration. However, the dependence on chirp rate is more complicated: for a fixed  $D_x$  the amplitude of  $\Delta\Gamma_e$  variations first increases with the chirp rate, and at larger  $b$  it starts decreasing. This non-monotonic behavior is caused by the interference of the energy stretch mechanism discussed in Sec. IV B: over the whole XUV pulse duration electrons with a wide spread of energies are created, which are differently affected by the laser field depending on their energies. At higher chirp rates the spectral width  $\Gamma_x$  of the pump pulse increases, which blurs the signature of its temporal structure. In addition, with increasing  $\Gamma_x$  the energy dependence of the cross-section [factor  $S(p)$  in Eq. (10)] becomes more and more important, whereby the laser-free photoelectron spectral width  $\Gamma_e^0$  increasingly strongly deviates from  $\Gamma_x$  (see also a discussion in Ref. [14] and the comment on Fig. 3 in the end of Sec. III).

The SSA is found to well reproduce the spectral width variations for  $\eta = bD_x/\Gamma_x^0 < 1.5$ , which covers a wide range of experimentally interesting pulses. For longer pulses or larger chirp rates it gives only a qualitative picture, see Fig. 7. The model systematically underestimates the amplitude of the  $\Delta\Gamma_e$  oscillations, with the largest discrepancy occurring when the energy sweep causes a compression of the spectrum. This has to be expected as the quantum interference between different processes that bring the excited electron to a given final state becomes most important in this case. The broadening of the spectra is reproduced much better; in particular, the time point at which the spectral width is maximal is predicted rather accurately. The numerical experiments, thus, suggest that the limitations of the SSA lie in treating the interaction with the laser field, i.e., in Eq. (6), whereas the heuristic description of the energy sweep by the instantaneous intensity distribution in Eq. (10) is quite reasonable.

In view of the complicated interplay between different broadening mechanisms and because the pulse width  $\Gamma_x$  is a non-linear function of both  $D_x$  and  $b$  the question arises whether a chirped pulse can be characterized by extracting only the gross parameter  $\Delta\Gamma_e$  from the streaking measurements. A more general but complicated procedure is to measure a complete spectrogram  $J(\epsilon, t_x)$  and decipher it with a FROG algorithm (frequency-resolved optical gating), which under certain conditions allows to reconstruct both the intensity profile and the phase of the pulse [20]. A physically more transparent way is to estab-

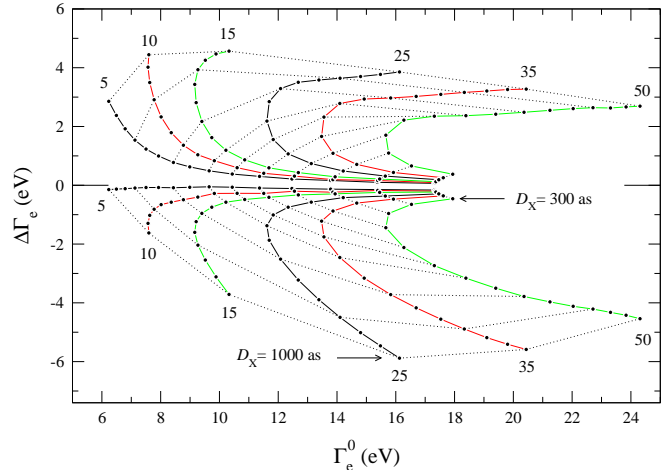


FIG. 8: (color online) Dependence of the laser-free spectral FWHM  $\Gamma_e^0$  and streaking broadening  $\Delta\Gamma_e$  on the duration  $D_x$  and chirp  $b$ . Positive  $\Delta\Gamma_e$  correspond to the release point  $t_x = -840$  as and negative to  $t_x = 840$  as. The  $b = \text{const}$  lines (solid lines) are labelled by chirp rate in the units of eV/fs. The dots in the lines are placed at equal intervals of 50 as between  $D_x = 300$  and 1000 as. Points of equal duration are connected by dotted lines.

lish a relation between gross features of the input pulse and the output spectrum and consider the release points at which the output is most sensitive to input. Following Ref. [3], we shall consider zero momentum transfer points.

In order to determine the temporal parameters  $b$  and  $D_x$  from the spectral characteristics  $\Gamma_e^0$  and  $\Delta\Gamma_e$  the input values must be presented in the output coordinates. The map in Fig. 8 shows  $b = \text{const}$  lines parametrized by  $D_x$  for the two zero momentum transfer points, see Fig. 4(b). The data are obtained with the exact TDSE. According to our calculations, neither the  $b = \text{const}$  lines nor the  $D_x = \text{const}$  ones intersect, which means that, in principle, both  $b$  and  $D_x$  can be determined from a laser-free EDC and a single streaked measurement (for one of the  $\Delta p = 0$  points). The sensitivity of output to input strongly varies over the map: the uncertainty of  $D_x$  increases with  $D_x$ , especially for small chirp rates, and at short durations the uncertainty of  $b$  increases. The complicated structure of the map implies that solution of the inverse problem requires a careful consideration of the photoexcitation process, as well as very accurate measurement of the EDCs.

## VI. SUMMARY

The main result of this work is the extension of the well known factorization  $J(\epsilon) \sim I(\epsilon)S(\epsilon)$  of the photoelectron spectrum by a single short pulse to laser assisted photoemission [as expressed by Eqs. (6), (7), and (10)]. This simple relation tells us that the laser free photoelectron spectrum is determined by the spectrum of the

exciting pulse but does not depend upon its temporal structure. In the streaking measurements it is just the temporal structure which is probed, and we have shown that the resulting spectrum depends on the intensity envelope, while the phase structure of the pump pulse is blurred. In the case of a Fourier limited pulse it enters only indirectly, as the relation between the temporal and the spectral extent of the pulse. In the case of a chirped pulse it is insufficient to know the time envelope and the spectrum. We have shown that this more complicated temporal structure can to a good approximation be treated in spirit of the formal instantaneous frequency by introducing an instantaneous spectral distribution and again neglecting the actual phase relations.

We have applied these considerations to calculating streaked spectra within the semiclassical superposition approximation. Although the concept of initial time-momentum distribution  $r_{\text{ini}}(p, t)$  lacks a rigorous physical meaning a function with the required properties can be constructed, which is capable of describing the lineshapes of streaked spectra for chirped pump pulses. In addition to the temporal structure of the pulse it takes into account its spectral extent, i.e., the fact that during the action of the pulse electrons are created in all states but with different rate. Both the temporal and the spectral factors are important for the shape of the streaked EDC, and the photon energy sweep, which both complicates the temporal structure and broadens the spectrum, provides a severe test of the SSA model. The model yields quantitatively correct results for a wide range of parameters and provides a useful basis for the understanding of the role of pulse parameters and properties of the electronic system. The latter are included through the energy dependent photoemission cross-section, which was found to strongly affect the lineshapes. The property of the model to decouple the semiclassical calculation of the time evolution of the system from the quantum-mechanical calculation of the dipole matrix elements makes it attractive for use for more complicated many-body systems, for which a consistent quantum-mechanical calculation is currently computationally infeasible: one can reason-

ably suppose that the present formalism would remain valid with a more advanced description of the excitation, see, e.g. Ref. [21] and references therein.

The main limitations of the model naturally come from its neglect of the quantum interference that accompanies the acceleration of the wave packet by the laser field. In the case considered this led to underestimated broadening and compression for sufficiently large pulse durations and chirp rates, but did not affect the qualitative picture.

The phenomenological function  $r_{\text{ini}}$  suggested in this paper differs from the time-momentum distribution  $r_0$  in the absence of the laser field in the two essential features: it discards the retardation of the final state population with respect to the pulse intensity profile and avoids negative values of the population rate. Thereby the function  $r_{\text{ini}}$  provides the most direct connection between the input pulse and the output EDC, and, moreover, the two aspects are found instrumental in reproducing the shape of the streaked EDCs within the SSA. This means, however, that in solving the inverse problem, i.e., obtaining information about the pump process from streaking measurements some essential features of the process may be lost.

We have shown that in the simplest case of a linear chirp the relation between the input pulse and output spectrum can be presented on a map that establishes a one to one correspondence between gross features of the input and the output. This means that provided a reliable theory of photoemission is available and the experimental resolution is high the pump pulse can be characterized by a few streak records.

### Acknowledgments

The authors gratefully acknowledge fruitful discussions with N.M. Kabachnik, A.K. Kazansky, E.V. Chulkov and P.M. Echenique. The work was supported by Ikerbasque (Basque Foundation for Science) and by the Innovationsfond Schleswig-Holstein.

- 
- [1] M. Hentschel, R. Kienberger, Ch. Spielmann, G.A. Reider, N. Milosevic, T. Brabec, P. Corkum, U. Heinzmann, M. Drescher, and F. Krausz, *Nature (London)* **414**, 509 (2001).
  - [2] M. Drescher, M. Hentschel, R. Kienberger, G. Tempea, Ch. Spielmann, G.A. Reider, P.B. Corkum, and F. Krausz, *Science* **291**, 1923 (2001).
  - [3] R. Kienberger, E. Goulielmakis, M. Uiberacker, A. Baltuska, V. Yakovlev, F. Bammer, A. Scrinzi, Th. Westerwalbesloh, U. Kleineberg, U. Heinzmann, M. Drescher, and F. Krausz, *Nature (London)* **427**, 817 (2004).
  - [4] A.L. Cavalieri, N. Müller, Th. Uphues, V.S. Yakovlev, A. Baltuska, B. Horvath, B. Schmidt, L. Blümel, R. Holzwarth, S. Hendel, M. Drescher, U. Kleineberg, P.M. Echenique, R. Kienberger, F. Krausz, and U. Heinzmann, *Nature (London)* **449**, 1029 (2007).
  - [5] F. Krausz and M. Ivanov, *Rev. Mod. Phys.* **81**, 163 (2009).
  - [6] J. Itatani, F. Quéré, G.L. Yudin, M.Yu. Ivanov, F. Krausz, and P.B. Corkum, *Phys. Rev. Lett.* **88**, 173903 (2002).
  - [7] M. Kitzler, N. Milosevic, A. Scrinzi, F. Krausz, and T. Brabec, *Phys. Rev. Lett.* **88**, 173904 (2002).
  - [8] A.K. Kazansky and N.M. Kabachnik, *J. Phys. B: At. Mol. Opt. Phys.* **39**, 5173 (2006).
  - [9] G.L. Yudin, S. Patchkovskii, P.B. Corkum, and A.D. Bandrauk, *J. Phys. B: At. Mol. Opt. Phys.* **40**, F93 (2007).
  - [10] E. Goulielmakis, V.S. Yakovlev, A.L. Cavalieri, M. Uiberacker, V. Pervak, A. Apolonski, R. Kienberger,



- U. Kleineberg, and F. Krausz, *Science* **317**, 769 (2007).
- [11] M.F. Kling and M.J.J. Vrakking, *Annu. Rev. Phys. Chem.* **59**, 463 (2008).
- [12] F. Quéré, Y. Mairesse, and J. Itatani, *J. Modern Optics* **52**, 339 (2005).
- [13] V.S. Yakovlev, F. Bammer, and A. Scrinzi, *J. Modern Optics* **52**, 395 (2005).
- [14] E.E. Krasovskii and M. Bonitz, *Phys. Rev. Lett.* **99**, 247601 (2007).
- [15] E. Goulielmakis, M. Uiberacker, R. Kienberger, A. Baltuska, V. Yakovlev, A. Scrinzi, Th. Westerwalbesloh, U. Kleineberg, U. Heinzmann, M. Drescher, and F. Krausz, *Science* **305**, 1267 (2004).
- [16] A.K. Kazansky and P.M. Echenique, *Phys. Rev. Lett.* **102**, 177401 (2009).
- [17] S. Bauch and M. Bonitz, *Phys. Rev. A* **78**, 043403 (2008).
- [18] S. Bauch and M. Bonitz, *Contrib. Plasma Phys.* (2009), in press, ArXiv: 0904.4855
- [19] M. Lewenstein, Ph. Balcou, M.Yu. Ivanov, A. L’Huillier, and P.B. Corkum, *Phys. Rev. A* **49**, 2117 (1994).
- [20] J. Gagnon, E. Goulielmakis, and V.S. Yakovlev, *Appl. Phys. B* **92**, 25 (2008).
- [21] D. Hochstuhl, K. Balzer, S. Bauch, and M. Bonitz, *Physica E*, in press.

## APPENDIX

We shall show that the simple relation  $J(\epsilon) \sim I(\epsilon)S(\epsilon)$  is obtained in the perturbational limit  $eA(t)/c \ll p$  of the time-dependent Schrödinger equation if one neglects the non-diagonal dipole matrix elements between the final states. In order to avoid the necessity of treating the final states as plane waves we consider a bound system (e.g., a quasi-continuum as in Fig. 1) with the unperturbed Hamiltonian  $\hat{H}_0 = -\Delta + V(x)$  and a time-dependent perturbation  $E(t) \hat{x}$ . Let us write the Schrödinger equation

$$i\dot{\psi}(t) = \left[ \hat{H}_0 + E(t) \hat{x} \right] \psi(t) \quad (\text{A.1})$$

in terms of the discrete spectrum of the eigenstates  $|j\rangle$  of the unperturbed operator,  $\hat{H}_0|j\rangle = \epsilon_j|j\rangle$ . The solution consists in finding the expansion coefficients  $a_j(t)$ :

$$|\psi(t)\rangle = \sum_{j=0}^{\infty} a_j(t) |j\rangle. \quad (\text{A.2})$$

The time-dependent Schrödinger equation then reads

$$i \sum \dot{a}_j(t) |j\rangle = \left[ \hat{H}_0 + E(t) \hat{x} \right] \sum a_j(t) |j\rangle. \quad (\text{A.3})$$

Let  $j = 0$  be the initial state, i.e.,  $a_0(0) = 1$  and  $a_j(0) = 0$  for  $j \neq 0$ . It can be shown that for a sufficiently weak potential  $V(x)$  the non-diagonal matrix elements of the position operator  $\hat{x}$  are much smaller than

the diagonal ones. Let us retain in Eq. (A.3) only the matrix elements  $d_{jj} = \langle j | \hat{x} | j \rangle$  and  $d_{j0} = \langle j | \hat{x} | 0 \rangle$ . Note that this approximation does not depend on the strength of the perturbing field  $E(t)$ . Its validity depends only on the properties of the system. Then the equations for different  $j$  separate:

$$i\dot{a}_j(t) = a_0(t)E(t)d_{j0} + a_j(t)[\epsilon_j + d_{jj}E(t)]. \quad (\text{A.4})$$

Let us write  $a_j(t)$  as a product  $a_j(t) = \exp[-i\epsilon_j t]\xi_j(t)$ . Then the equation for  $\xi_j(t)$  is

$$i\dot{\xi}_j(t) = \exp[i\omega_{j0}t]\xi_0(t)E(t)d_{j0} + \xi_j(t)E(t)d_{jj}. \quad (\text{A.5})$$

Here  $\omega_{j0} = \epsilon_j - \epsilon_0$ . The solution of Eq. (A.5) is

$$\begin{aligned} \xi_j(t) = & -i \int_{-\infty}^t dt' \xi_0(t') E(t') d_{j0} \exp[i\omega_{j0}t'] \\ & \times \exp \left[ id_{jj} \int_t^{t'} E(t'') dt'' \right], \end{aligned} \quad (\text{A.6})$$

or, in terms of vector potential  $A(t)$ ,

$$\begin{aligned} \xi_j(t) = & -i \int_{-\infty}^t dt' \xi_0(t') E(t') d_{j0} \exp[i\omega_{j0}t'] \\ & \times \exp[id_{jj}(A(t') - A(t))]. \end{aligned} \quad (\text{A.7})$$

At this point we introduce the requirement that the perturbation be small. Its implication is twofold: first, for  $A(t) \rightarrow 0$  the initial state can be considered unaffected by the electric field, so that  $\xi_0(t') = 1$ . Second, the phase  $d_{jj}(A(t') - A(t))$  can be neglected compared to  $\omega_{j0}t'$ . Then  $\xi_j(t)$  reduces to the Fourier transform  $E(\omega)$  of the XUV pulse multiplied by the dipole matrix element  $d_{j0}$ :

$$\xi_j(t) = -i d_{j0} \int_{-\infty}^t dt' E(t') \exp[i\omega_{j0}t']. \quad (\text{A.8})$$

The photoelectron spectrum after the pulse is over  $J(\omega_{j0}) = |\xi_j(D_x/2)|^2$  is then a product of the photoemission cross-section  $S(\omega_{j0}) = |d_{j0}|^2$  and the intensity spectrum  $I(\omega_{j0}) = |E(\omega_{j0})|^2$ . (Of course, Eq. (A.8) can be applied to any  $t$ , i.e., it describes the evolution of the spectrum, too.) This result is also obtained in the perturbational limit of the equations of Ref. [19], but in the present derivation the assumption of plane-wave-like final states is recast as the approximation of vanishing non-diagonal elements of the perturbation between final states.